Characterization of the Magnitude and Kinetics of Xanthine Oxidase-Catalyzed Nitrate Reduction: Evaluation of Its Role in Nitrite and Nitric Oxide Generation in Anoxic Tissues

Haitao Li, Alexandre Samouilov, Xiaoping Liu, and Jay L. Zweier*

Center for Biomedical EPR Spectroscopy and Imaging and the Davis Heart and Lung Research Institute, The Ohio State University College of Medicine, Columbus, Ohio 43210, and the Electron Paramagnetic Resonance Center, The Johns Hopkins University School of Medicine, 5501 Hopkins Bayview Circle, Baltimore, Maryland 21224

Received July 1, 2002; Revised Manuscript Received October 31, 2002

ABSTRACT: In addition to nitric oxide (NO) generation from specific NO synthases, NO is also formed during anoxia from nitrite reduction, and xanthine oxidase (XO) catalyzes this process. While in tissues and blood high nitrate levels are present, questions remain regarding whether nitrate is also a source of NO and if XO-mediated nitrate reduction can be an important source of NO in biological systems. To characterize the kinetics, magnitude, and mechanism of XO-mediated nitrate reduction under anaerobic conditions, EPR, chemiluminescence NO-analyzer, and NO-electrode studies were performed. Typical XO reducing substrates, xanthine, NADH, and 2,3-dihydroxybenz-aldehyde, triggered nitrate reduction to nitrite and NO. The rate of nitrite production followed Michaelis−Menten kinetics, while NO generation rates increased linearly following the accumulation of nitrite, suggesting stepwise-reduction of nitrate to nitrite then to NO. The molybdenum-binding XO inhibitor, oxypurinol, inhibited both nitrite and NO production, indicating that nitrate reduction occurs at the molybdenum site. At higher xanthine concentrations, partial inhibition was seen, suggesting formation of a substrate-bound reduced enzyme complex with xanthine blocking the molybdenum site. The pH dependence of nitrite and NO formation indicate that XO-mediated nitrate reduction occurs via an acid-catalyzed mechanism. With conditions occurring during ischemia, myocardial xanthine oxidoreductase and nitrate levels were determined to generate up to 20 μM nitrite within 10−20 min that can be further reduced to NO with rates comparable to those of maximally activated NOS. Thus, XOR catalyzed nitrate reduction to nitrite and NO occurs and can be an important source of NO production in ischemic tissues.

Nitric oxide is a free radical that exerts a large number of important regulatory biological functions and also plays an important role in the pathogenesis of cellular injury. NO[1] synthesis was discovered in macrophages, endothelial cells, and neuronal cells (*1*−*4*). A group of enzymes were identified, nitric oxide synthases (NOSs), which metabolize arginine to citrulline with the formation of NO (*5*, *6*). Although NOS had been generally considered to be the primary source of NO in biological systems, there have also been reports that NOS-independent NO generation occurs from nitrite or nitrate in various ways. Benjamin and colleagues reported in 1994 that acidification of nitrite releases NO in the stomach (*7*). In 1994, Lundberg et al. also reported measuring high levels of NO expelled in air from the stomach of humans (*8*), and subsequently in 1997, they reported that NO is derived from nitrate in infected urine (*9*). Previous studies have also demonstrated that NOS-independent generation of NO from nitrite occurs in ischemic tissues such as the heart, demonstrating that nitrite can be a source rather than a product of NO particularly under acidic conditions (*10*−*12*). Recently it has been reported that XO catalyzes reduction of nitrite to NO under hypoxic conditions (*13*−*15*) and the magnitude and kinetics of this process have been characterized (*16*). While it is clear that nitrite can be an important source of NO in cells and tissues, it has been assumed that nitrate is an inert end product that cannot be a source of NO in mammalian cells.

Xanthine oxidase (XO) is a ubiquitous enzyme in mammalian cells that plays a variety of important roles in normal physiology and disease. XO has a critical role in purine and pyrimidine catabolism, catalyzing the oxidation of hypoxanthine to xanthine and xanthine to uric acid. It also reduces oxygen to superoxide and hydrogen peroxide and is a key enzyme responsible for oxidative cellular injury (*17*). XO has been shown to have a central role in the process of injury that occurs upon reoxygenation of hypoxic cells and tissues (*18*−*20*). It has structural similarity to bacterial nitrate or nitrite reductase (*13*). Early studies showed that xanthine oxidoreductase (XOR) has the ability to catalyze the reduction of nitrate to nitrite under anaerobic conditions (*21*−*24*). This could be particularly important since nitrates are ubiquitous in biological tissues and are normally present at

* Corresponding author. Address: 110G Davis Heart & Lung Research Institute, 473 West 12th Avenue, Columbus, OH 43210-1252. E-mail: zweier-1@medctr.osu.edu.

[1] Abbreviations: XO, xanthine oxidase; XOR, xanthine oxidoreductase; XDH, xanthine dehydrogenase; X, xanthine; NADH, nicotinamide adenine dinucleotide; DBA, 2,3-dihydroxybenzaldehyde; NO, nitric oxide; MGD, *N*-methyl-D-glucamine dithiocarbamate; EPR, electron paramagnetic resonance; DPI, diphenyleneiodonium chloride; FAD, flavin−adenine dinucleotide; Mo, molybdenum.

10.1021/bi026385a CCC: $25.00
Published on Web 01/04/2003

high levels reaching millimolar concentrations following inflammation or treatment with NO-donating vasodilator drugs (*25*). Recent work further suggested that XO is capable of catalyzing the reduction of nitrate to NO under hypoxic conditions in the presence of NADH (*14*), but a number of important questions have remained regarding the mechanism, substrate specificity, and the magnitude of this process in biological systems. Fundamental questions remain regarding the kinetics of this process and its biological importance.

To characterize this XO-catalyzed nitrate reduction pathway, along with its mechanism, substrate dependence, and quantitative importance in biological systems, electron paramagnetic resonance (EPR) spectroscopy, chemiluminescence NO analyzer, and NO electrode studies were performed. The rate of nitrite production followed Michaelis−Menten kinetics with xanthine, NADH or 2,3-dihydroxybenzaldehyde serving as the reducing substrates, while NO generation rate increased linearly with the increase of nitrite formed from nitrate indicating stepwise reduction to nitrite and then to NO. Nitrate reduction to nitrite as well as nitrite reduction to NO occurred at the molybdenum site. The K_m values for nitrate, NADH, and xanthine were determined enabling prediction of the magnitude of nitrite and NO formation with delineation of the quantitative importance of this process in biological systems.

MATERIALS AND METHODS

Materials. Xanthine oxidase from buttermilk (xanthine: oxygen oxidoreductase; EC1.1.3.22), xanthine, oxypurinol, diphenyleneiodonium chloride (DPI), N^{ω}-nitro-L-arginine, sodium nitrate, sodium nitrite, β-nicotinamide adenine dinucleotide (β-NADH), and 2,3-dihydroxybenz-aldehyde (DBA) were obtained from Sigma. *N*-Methyl-D-glucamine dithiocarbamate (MGD) was synthesized using carbon disulfide and *N*-methyl-D-glucamine, as described previously(*26*). Ferrous ammonium sulfate was purchased from Aldrich Chemical Co (99.997%). ^{15}N-nitrate was obtained by Cambridge Isotope Laboratories, Inc. Hank's Balanced Salt Solution (HBSS) and Dulbecco's Phosphate Buffered Saline (PBS) were obtained from Gibco Life Technologies.

EPR Spectroscopy. EPR measurements were performed using a Bruker ER 300 spectrometer operating at X-band. Measurements were performed in a flat cell using a TM_{110} microwave cavity at ambient temperature with a modulation frequency of 100 kHz, modulation amplitude of 2.5 G, microwave power of 20 mW. NO formation was measured by spin trapping using the ferrous iron complex of *N*-methyl-D-glucamine dithiocarbamate (MGD), Fe−MGD, which forms a stable, water-soluble mononitrosyl adduct, $(MGD)_2-Fe^{2+}-NO$, that exhibits a characteristic triplet EPR spectrum at $g = 2.04$ and $a_N = 12.8$. Solid ferrous ammonium sulfate and MGD (molar ratio 1:5) were added to the deoxygenated (argon-purged) solution with a final concentration 2 mM in iron (*12*).

Chemiluminescence Measurements. The rate of the NO production was measured using a Sievers 270B nitric oxide analyzer interfaced through a DT2821 A to D board to a PC. In the analyzer, NO is reacted with ozone forming excited-state NO_2, which emits light. Mixing of reagents and separation of NO from the reaction mixture were done at controlled temperature in a glass-purging vessel equipped with heating jacket. An ice−water cooling condenser was attached to the top of the vessel to reduce the outflow of vapors during purging. Additionally, an ice-cooled chemical trap filled with 1.0 M NaOH was placed between the purging vessel and NO analyzer. The release of NO was quantified by analysis of the digitally recorded signal from the photomultiplier tube using specially designed data acquisition and analysis software developed in our laboratory.

The chemiluminescence assay for measurement of nitrite in the solution utilizes the reduction of nitrite to NO under conditions of acidic pH in the presence of the reducing agent KI. Calibration of the magnitude of nitrite and NO production was determined from the integral of the signal over time compared to that from nitrite concentration standards added to glacial acetic acid containing 1% KI (*12*).

Electrochemical Measurements. Electrochemical measurements of NO generation from XO were carried out at 37 °C in a deaerated electrochemical vial using a CHI 832 electrochemical detector with a Faraday Cage (CH Instruments, Inc., Cordova, IN) and WPI NO electrode (World Precision Instruments, Sarasota, FL). To remove oxygen, the reaction solutions and the measurement chambers were purged with argon for 15 min before each experiment. The electrochemical detector continuously recorded the current through the working electrode, which is proportional to the NO concentration in the solution. The sensor was calibrated before and after experiments with known concentrations of NO, using NO equilibrated solutions.

EPR Trapping of NO in Heart Tissue. Male Sprague−Dawley rats (250−300 g) were heparinzed with 500 units of heparin and anesthetized with intraperitoneal pentobarbital at a dose of 30−35 mg/kg. The hearts were excised and cut into small pieces (~0.01 g/piece), and then rinsed with HBSS solution to wash away blood and intrinsic nitrite/nitrate. This heart tissue, totaling 1 g, suspended in 3 cm^3 HBSS was purged with argon and incubated with ^{15}N nitrate (1mM) and Fe-MGD, 2 mM in Fe prepared as above. The reaction mixture was maintained at 37 C in a glass-purging vessel equipped with heating jacket. After incubation, the solution was cooled on ice and transferred to a flat cell, and EPR spectra were measured as described above.

Statistical Analysis. Values are expressed as mean ± SD of at least three repeated measurements and statistical significance of difference was evaluated by students t-test. A *P* value of 0.05 or less was considered to indicate statistical significance.

RESULTS

XO-Mediated NO Generation from Nitrate. NO is paramagnetic and binds with high affinity to the water-soluble spin trap, $Fe^{2+}-MGD$, forming a mononitrosyl iron complex with characteristic triplet spectrum at $g = 2.04$ with hyperfine splitting $a_N = 12.8$. From the intensity of the observed spectrum, quantitative measurement of NO generation can be performed(*10*, *11*). This technique was applied to measure nitrate-mediated NO generation under anaerobic conditions. In the absence of nitrate, no signal was seen from mixtures of XO (0.1 mg/mL) and its reducing substrate xanthine (0.1 mM) (Figure 1 A). In the absence of XO, nitrate (10 mM) and xanthine (100 μM) also did not give rise to any signal (Figure 1 B). Similarly, in the absence of the enzyme, no

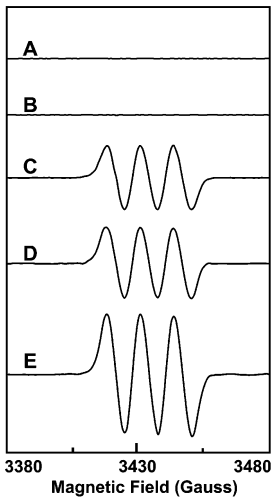

FIGURE 1: EPR measurement of NO generation from XO and nitrate. Spectra are shown of the $(MGD)_2-Fe^{2+}-NO$ adduct formed in solutions of 2 mM $(MGD)_2-Fe^{2+}$ complex in PBS buffer (pH 7.4) with (A) 0.1 mg/mL XO and 100 μM xanthine, (B) 10 mM nitrate and 100 μM xanthine, (C) 10 mM nitrate, 0.1 mg/mL XO, and 5 mM NADH, (D) 10 mM nitrate, 0.1 mg/mL XO, and 100 μM xanthine, or (E) 10 mM nitrate, 0.1 mg/mL XO, and 0.5 mM 2,3-dihydroxybenzaldehyde. Spectra A−C were obtained after incubation for 4 h at 37 °C under anaerobic conditions, while D and E were after only 2 h.

signal was seen from nitrite and NADH or DBA (data not shown). However, upon mixing of nitrate, XO and its reducing substrates NADH (5 mM) or xanthine (100 μM), or DBA (0.5 mM), a large NO signal was seen (Figure 1C,D,E). Thus, all of the typical types of XO reducing substrates, including NADH, 2,3-dihydroxybenz-aldehyde (DBA), and xanthine, acted as electron donors for XO-catalyzed nitrate reduction and triggered NO generation under anaerobic conditions. We observed, however, that nitrate reduction was much slower and required a much longer time (xanthine and DBA, 2 h; NADH, 4 h) to generate an observed NO signal than the previously characterized process of nitrite reduction (*16*). In addition, at least 10-fold higher nitrate concentrations were required to produce an NO signal of comparable intensity to that formed by XO-catalyzed nitrite reduction (*16*).

To further confirm the existence of XO-catalyzed NO generation and avoid any possible perturbation caused by the spin trap, studies were performed using a specific electrochemical NO sensor. Prior to the addition of XO, no detectable NO generation was seen from nitrate (1.0 mM) in the presence of DBA (0.5 mM), xanthine (50 μM), or NADH (2.0 mM). However, after addition of XO (0.04 mg/mL), NO generation was triggered from DBA, xanthine, or NADH (Figure 2A−C). The magnitude and rate of NO generation in the presence of DBA (Figure 2A) or xanthine (Figure 2B) was considerably higher than that with NADH (Figure 2C). Thus, both EPR spin trapping and NO electrode studies demonstrated that XO could generate NO in the presence of substrates that reduce the enzyme.

The measurement of NO generation by electrochemical method was used to determine the NO accumulation in the liquid phase. However, it is inevitable that some NO can escape to the atmosphere during the experiment. To quantitate the rate of XO-mediated NO generation, further studies were performed using a chemiluminescence NO analyzer.

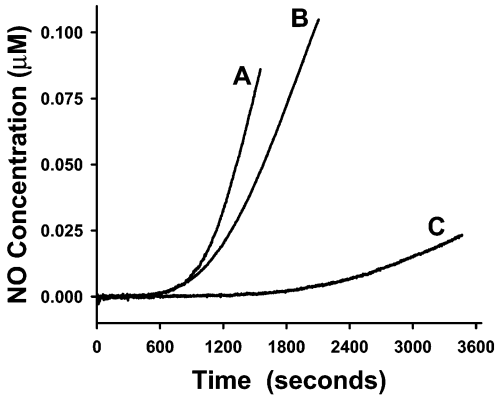

FIGURE 2: Electrochemical measurement of NO generation from XO and nitrate. The time course of NO generation was measured using an electrochemical NO sensor under anaerobic conditions at 37 °C in PBS, pH 7.4, from 1.0 mM nitrate and XO (0.04 mg/mL) in the presence of (A) 2,3-dihydroxybenzaldehyde (0.5 mM), (B) xanthine (50 μM), and (C) NADH (2.0 mM).

NO was purged from the solution with argon gas. It has been shown that rate of NO generation by XO-catalyzed nitrite reduction follows classical Michaelis−Menten kinetics (*16*). In contrast, XO-mediated NO generation rates from nitrate increase as a function of time with the substrates DBA (Figure 3A), xanthine (Figure 3B), or NADH (Figure 3C). In all cases, unusual self-accelerating behavior was observed. With DBA (0.5 mM), XO (0.04 mg/mL) triggered NO generation that increased linearly as a function of time, and the slope of NO generation rates increased as a function of nitrate concentration (Figure 3A). In the presence of 10 μM xanthine (Figure 3B) or 2.0 mM NADH (Figure 3C), linearly increasing rates of NO generation were initially observed following addition of XO, and the rate of NO generation also increased as a function of nitrate concentration. Of note, a much higher rate of XO-mediated NO generation was seen with DBA or xanthine than with NADH.

Kinetics of XO-Catalyzed Nitrite Generation by Nitrate Reduction. Early studies have shown that XOR has the ability to catalyze the reduction of nitrate to nitrite under anaerobic conditions (*21*−*24*). To investigate the mechanism of XOR catalyzed nitrite generation from nitrate as well as its substrate specificity and the role of nitrite production in the process of NO generation, the rate of nitrite formation derived from XO catalyzed nitrate reduction was measured under anaerobic conditions. In the presence of 1.0 mM nitrate and reducing substrates DBA (0.5 mM), X (10 μM), or NADH (2.0 mM), after addition of XO, 0.1 mL of the reaction mixture was sampled every minute, and its nitrite concentration was determined by NO analyzer with reduction of nitrite to NO using 1% KI under acidic conditions. In these experiments, a large amount of nitrite generation was triggered by DBA, xanthine, or NADH (Figure 4). The linear increase in nitrite concentrations in the reaction mixture demonstrated that nitrite generation rates were almost constant, contrary to the linearly rising NO generation rates observed in Figure 3.

The rates of nitrite generation can be determined from the ratio of nitrite concentration to reaction time. The concentration dependences of nitrite production on reducing substrates DBA or NADH were first determined in the presence of a fixed nitrate concentration of 1.0 mM. DBA or NADH acted as electron donors to support XO-catalyzed nitrate reduction,

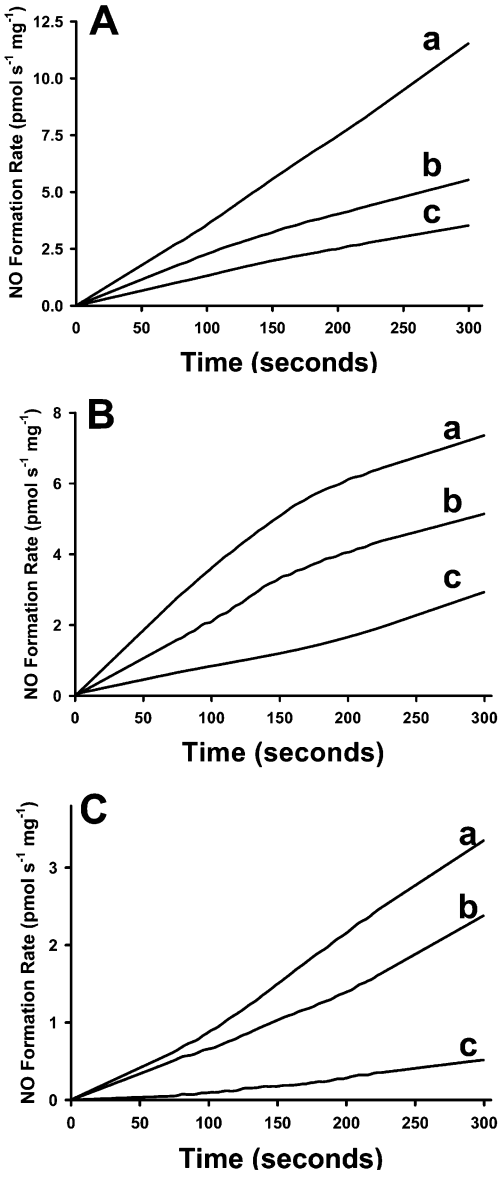

FIGURE 3: Time course of NO generation from XO-catalyzed nitrate reduction. Measurements were performed using a chemiluminescence NO analyzer under anaerobic conditions at 37 °C in PBS, pH 7.4. Time courses of NO generation were measured from the following: (A) 0.5 mM 2,3-dihydroxybenz-aldehyde, and 0.04 mg/mL XO in the presence of (a) 1.0 mM, (b) 0.5 mM, and (c) 0.25 mM nitrate; (B) 10 μM xanthine and 0.04 mg/mL XO in the presence of (a) 2.0 mM, (b) 1.0 mM, and (c) 0.5 mM nitrate; (C) 2.0 mM NADH and 0.1 mg/mL XO in the presence of (a) 10.0 mM, (b) 5.0 mM, and (c) 1.0 mM nitrate.

and each of these reactions followed Michaelis−Menten kinetics with correlation coefficient γ^2 >99% (Figure 5A,B). For each reducing substrate, the apparent values of K_m and V_{max} were determined by fitting the data to the Michaelis−Menten equation, and the values for each reducing substrate are shown inside each curve. For each of these reducing substrates, the rate of XO-mediated nitrite formation was also determined as a function of nitrate concentration (Figure 5 C, D). Again, typical Michaelis−Menten kinetics were observed (correlation coefficient γ^2 > 99%) as a function of nitrate concentration, and the apparent K_m and V_{max} values are shown inside each curve. From this kinetic data, it is possible to predict the magnitude of XO-catalyzed nitrite formation as a function of nitrate and reducing substrate

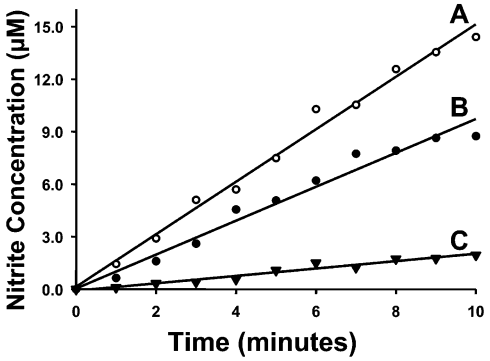

FIGURE 4: Time course of nitrite production from XO-catalyzed nitrate reduction. The reaction mixture was sampled 0.1 mL every minute, and nitrite concentration was measured by NO analyzer with nitrite reduction to NO using 1% KI under acidic conditions. Measurements were performed in the presence of (A) 0.5 mM 2,3-dihydroxybenzaldehyde, 0.04 mg/ml XO, and 1 mM nitrate, (B) 10 μM xanthine, 0.04 mg/mL XO, and 1.0 mM nitrate, and (C) 2.0 mM NADH, 0.1 mg/mL XO, and 1.0 mM nitrate. The points show the measured experimental values, and the line shows the linear regression fit of the data points with correlation coefficient γ^2 > 0.95.

concentration and to determine the quantitative importance of this mechanism of nitrite generation and its subsequent NO generation in a given biological system where these substrate levels are known.

Inhibitive Effect of High Xanthine Levels on NO Generation. It has been reported that excess xanthine (>100 μM) can exert inhibition of XO catalytic function due to binding of xanthine to reduced forms of the enzyme generated in the steady-state process of XO-catalyzed oxygen reduction. This kind of substrate-bound reduced XO complex inhibits intramolecular electron transport from the molybdenum center to FAD (*27*, *28*). Our previous study also showed that at higher xanthine concentrations, partial inhibition of XO-catalyzed NO generation from nitrite reduction occurs, suggesting the formation of a substrate-bound reduced enzyme complex with xanthine blocking the molybdenum site. In view of the questions regarding the role and potency of xanthine as a reducing substrate for the process of XO-mediated nitrate reduction to nitrite, NO analyzer studies were performed to detect XO-catalyzed nitrite generation in the presence of 0.1−1.0 mM nitrate. Measuring the average rate of nitrite generation over five minutes, a process of xanthine-stimulated nitrite generation was seen in which higher concentrations of xanthine showed significant concentration-dependent inhibition of nitrite formation (Figure 6). Maximum rates of nitrite generation of 0.96, 0.19, 0.26, 0.44, and 0.48 nmol s^{-1} mg^{-1} were observed for 0.1, 0.2, 0.4, 0.8, and 1.0 mM nitrate, respectively, at xanthine concentrations ranging from 5 to 20 μM. With further increase in xanthine levels, progressive inhibition was seen, consistent with concentration-dependent inhibition (Figure 6). From fitting of the data in Figure 6, K_i was calculated to be 80 μM. These results suggest that a xanthine-reduced XO complex is formed and inhibits XO-catalyzed nitrate reduction by binding to reduced forms of the enzyme, in turn blocking the binding of nitrate to the molybdenum site.

Effects of pH on XO-Catalyzed NO Generation. Under ischemic conditions, marked intracellular acidosis occurs, and pH values in tissues, such as the heart, can fall to levels of 6.0 or below (*11*). To assess the NO formation under different

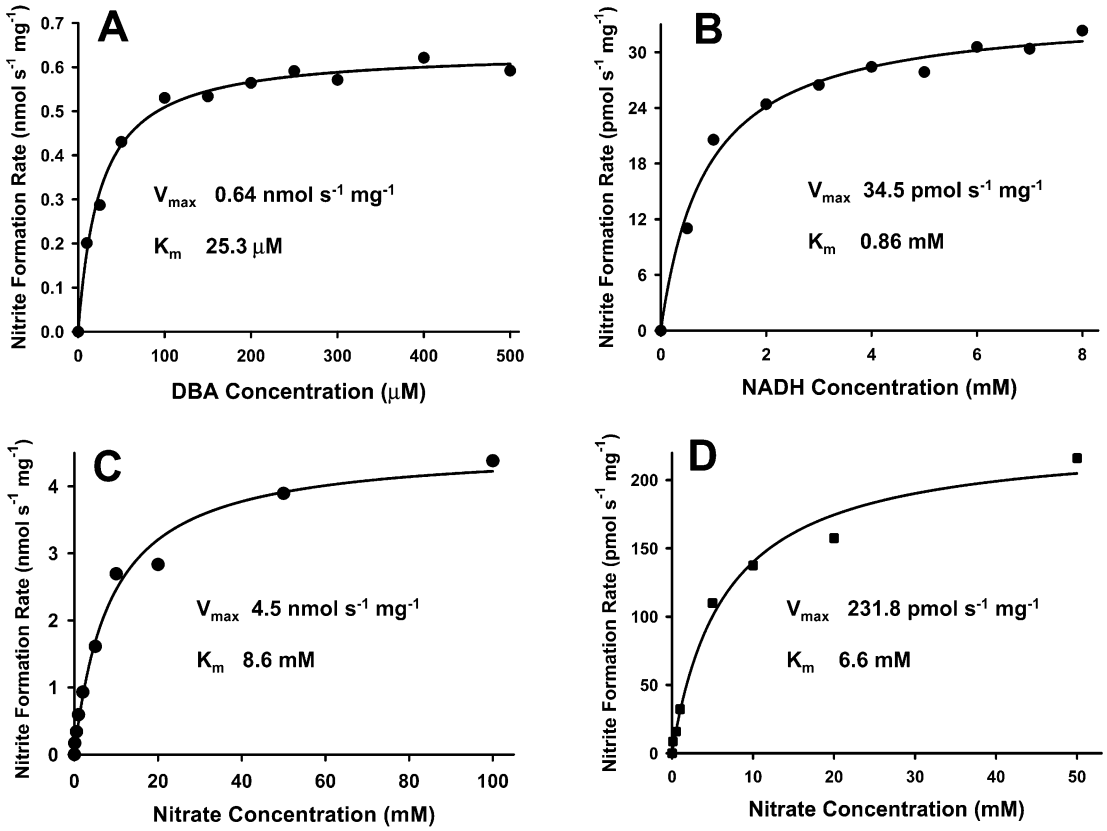

FIGURE 5: Kinetics of XO-mediated nitrite generation as a function of reducing substrate or nitrate concentration. The initial rates of nitrite production were measured from the slope of the graph of nitrite concentration versus time. Panel A shows the effect of 2,3-dihydroxybenzaldehyde (DBA) on the rate of nitrite generation from 0.04 mg/mL XO and 1.0 mM nitrate. Panel B shows the effect of NADH on the rate of nitrite generation from 0.04 mg/mL XO and 1 mM nitrate. Panel C shows the rate of nitrite generation by 0.04 mg/mL XO, 0.5 mM 2,3-dihydroxybenzaldehyde in the presence of 0.1−100 mM nitrate. Panel D shows the rate of nitrite generation by 0.1 mg/mL XO and 2.0 mM NADH in the presence of 0.1−50 mM nitrate. For each of these graphs, the corresponding fitting (solid lines), K_m and V_{max} data were obtained using the Michaelis−Menten equation.

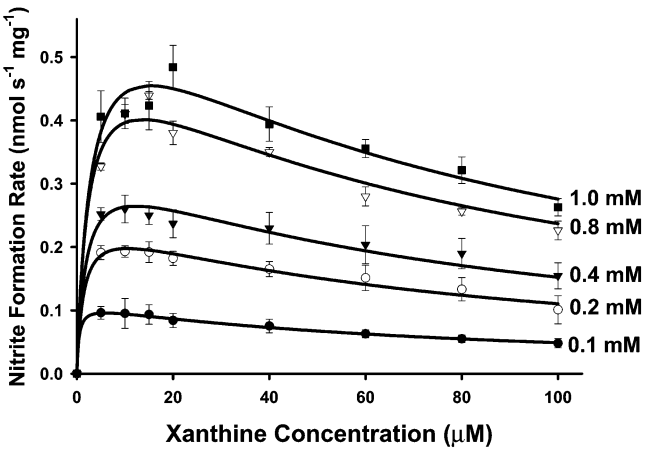

FIGURE 6: Inhibition of XO-mediated nitrite generation by high xanthine concentrations. Rates of nitrite generation as a function of xanthine concentration were measured by chemiluminescence NO analyzer with 0.1, 0.2, 0.4, 0.8, or 1.0 mM nitrate and 0.04 mg/mL of XO. Maximum rate of NO generation was seen with low xanthine concentrations followed by progressive inhibition at high substrate levels. The points show the measured experimental values with SD bars, and the line shows the fit of the data to the rate equation with competitive inhibition, eq 9. A good fit was observed with correlation coefficient $\gamma^2 > 0.97$.

physiological or pathological conditions and to further characterize the mechanism of XO-catalyzed nitrate reduction, experiments were performed to measure the effect of different pH values on the magnitude of nitrite and NO generation. As shown in Figure 7, for each of the substrates xanthine, NADH, and 2,3-dihydroxybenzaldehyde, it was observed that maximum XO-catalyzed nitrite and NO generation occur at pH 5. When the pH was decreased to 4 or increased above 5, a prominent decrease in the rate of nitrite and NO formation was observed.

Determination of the Mechanism and Reaction Site of Nitrite Reduction. The effects of site-specific inhibition of XO were studied to investigate the reaction sites involved in the process of the XO-catalyzed nitrate reduction with different reducing substrates. Oxypurinol binds to the molybdenum site of XO. It was observed that oxypurinol inhibited XO-catalyzed nitrate reduction, regardless of the type of reducing substrate present. Near total inhibition of nitrite generation was seen in the presence of either xanthine or NADH (Figure 8). Because oxypurinol inhibits substrate binding at the molybdenum site of the enzyme, this suggests that nitrate binds to the reduced molybdenum site. DPI, which acts at the FAD site, inhibited XO-dependent nitrate reduction only when NADH was used as the reducing substrate, and it did not inhibit nitrite generation when xanthine was used (Figure 8). This suggests that NADH donated electrons to FAD, and then electrons are transported back to reduce the molybdenum that, in turn, reduces nitrate to nitrite. When xanthine or aldehydes are the electron donors, both XO reduction (by xanthine or aldehydes) and oxidation (by nitrate) take place at the molybdenum site, so that only

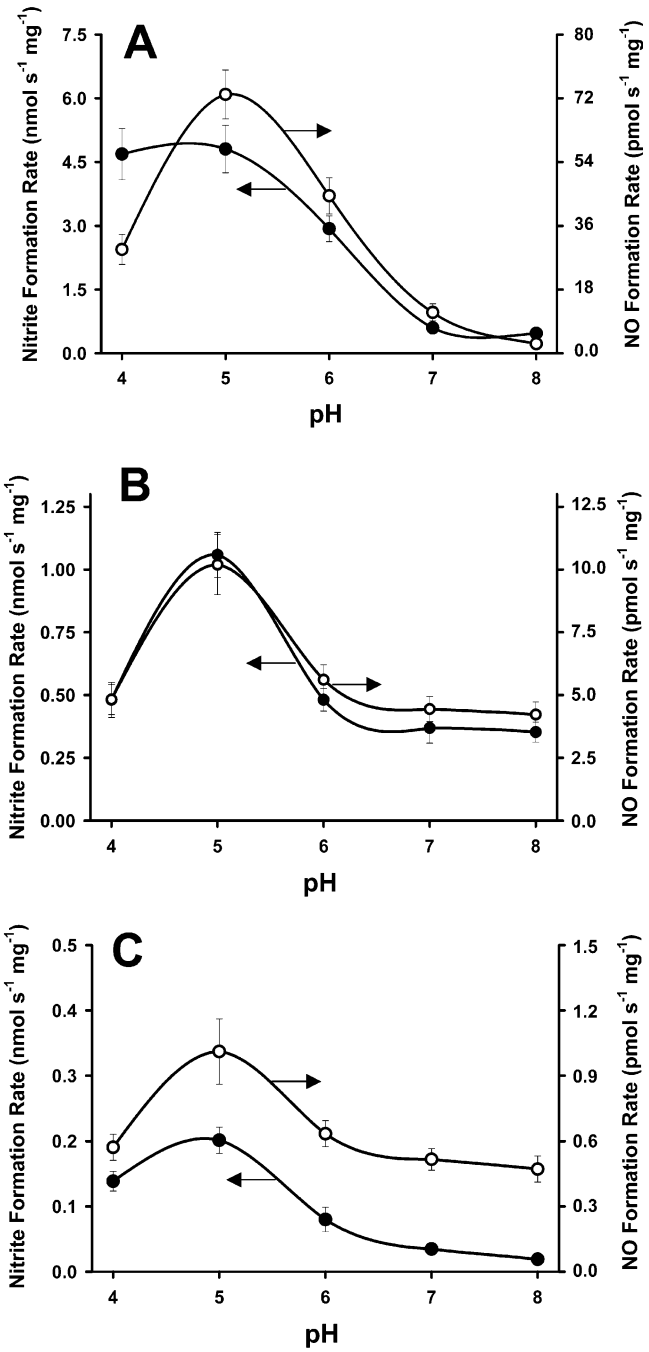

FIGURE 7: Effect of pH on nitrite and NO generation rate. Mean rates of nitrite generation 5 min after incubation were determined by chemiluminescence NO analyzer as described in Figure 5. Measurements in panel A were performed with 1.0 mM nitrate, 0.04 mg/mL of XO in the presence of 0.5 mM 2,3-dihydroxybenzaldehyde. Panel B shows the data for 1.0 mM nitrate, 0.04 mg/mL XO in the presence of 10 μM xanthine, while panel C shows that for 1.0 mM nitrate, 0.04 mg/mL XO in the presence of 2.0 mM NADH.

oxypurinol could inhibit XO-dependent nitrite formation-(*16*).

XO-Mediated NO Generation from Nitrate in Heart Tissue. To determine if nitrate can be reduced to form NO in hypoxic tissues and to ascertain the role of XO in this process, studies were performed in which heart tissue was subjected to hypoxia in the presence of isotopically labeled nitrate. Rat heart tissue was isolated and cut into pieces (~10 mg) suspended in HBSS and purged with argon. The tissue was

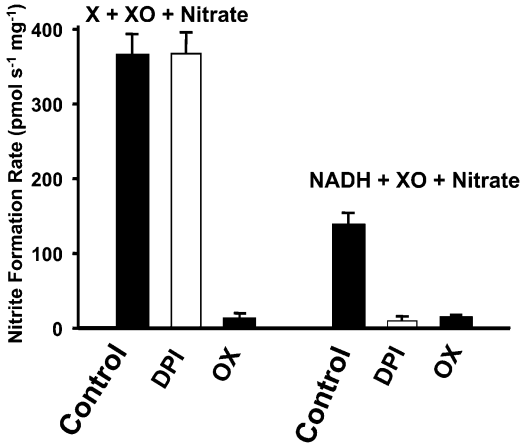

FIGURE 8: Effect of site-specific inhibitors on XO-mediated nitrite formation. Rates of nitrite generation were measured by chemiluminescence NO analyzer as described in Figure 5. For the left set of bars, experiments were performed with 1.0 mM nitrate, 10 μM xanthine and 0.04 mg/mL XO and for the right set of bars, with 1.0 mM nitrate, 2.0 mM NADH, and 0.1 mg/mL XO. Control, without inhibitor, DPI, 20 μM, oxypurinol, 20 μM.

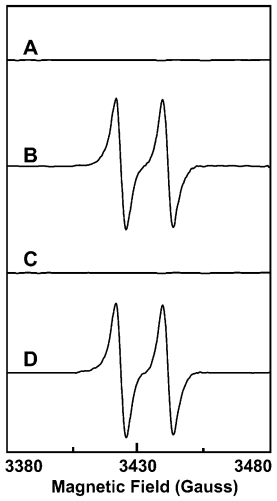

FIGURE 9: EPR measurement of NO generation from ^{15}N-nitrate in heart tissue. Spectra are shown of the $(MGD)_2-Fe^{2+}-{}^{15}NO$ adduct formed in solutions of 2 mM $(MGD)_2-Fe^{2+}$ complex in HBSS buffer (pH 7.4) with (A) 1mM ^{15}N-nitrate, (B) 1 mM nitrate and 1 g heart tissue, (C) 1 mM nitrate, 1 g heart tissue and 50 μM oxypurinol, and (D) 1 mM nitrate, 1 g heart tissue, and 1 mM Nω-nitro-L-arginine. Spectra shown in A−D were obtained after incubation for 1 h at 37 °C under anaerobic conditions.

rinsed to prevent foaming of blood in the tissue during the purging and to minimize the intrinsic nitrite/nitrate. NO production from ^{15}N-nitrate in anoxic heart tissue was measured by EPR spectroscopy. ^{15}NO gives a characteristic doublet $^{15}NO-Fe^{2+}-$MGD spectrum, rather than the triplet observed with natural abundance ^{14}NO, enabling direct and selective detection of nitrate-derived NO formation. In the absence of added nitrate, no significant signal was seen from heart tissue (Figure 9 A). However, upon addition of ^{15}N−nitrate, a large NO signal was seen (Figure 9 B). With addition of the XO inhibitor oxypurinol, the $^{15}NO-$Fe-MGD signal was quenched (Figure 9 C), while with the NOS-inhibitor N$^{\omega}$-nitro-L-arginine, no inhibition was seen (Figure 9 D). Thus, XO-mediated nitrate reduction is a prominent source of NO in the hypoxic tissue.

DISCUSSION

In addition to the formation of NO from specific NOS enzymes, it is clear that nitrate and nitrite derived from either NO metabolism or dietary sources can be an important source of NO formation, particularly under conditions of limited tissue perfusion and resulting acidosis. XO-catalyzed reduction of nitrite to NO has been recently reported, and the magnitude and kinetics of this XO-mediated nitrite reduction has been determined. Under conditions occurring during no-flow ischemia, myocardial XO and nitrite levels were found to be sufficient to generate NO levels comparable to those produced from NO synthase (*16*). However, nitrite concentrations in plasma and urine are usually only a small fraction (<5%) of the nitrate concentrations, and nitrite is unstable with rapid oxidation to nitrate in blood (*29*). XO-mediated nitrite generation from nitrate was first recognized in 1924 and was studied in early reports (*21*−*24*). Recently, Millar et al. reported measuring NO generation by XO-mediated nitrate reduction in the presence of NADH (*14*). However, questions remain about the mechanism, substrate specificity, and the relationship of nitrite and NO generation in the process of nitrate reduction, as well as the magnitude and quantitative importance of this process in biological systems. Therefore, we performed a series of studies using EPR spectroscopy, chemiluminescence NO analyzer, and NO electrode techniques to measure the magnitude and kinetics of nitrite and NO formation that arises from XO-mediated nitrate reduction.

Data obtained using each of these three methods confirmed that XO does reduce nitrate to NO under anaerobic conditions. It was observed that each of the typical reducing substrates xanthine, DBA, and NADH could act as electron donors to support this XO-mediated nitrite reduction (Figures 1−3). The results of these studies, along with the inhibition seen with oxypurinol, suggested that reduced XO was the direct electron donor to nitrate, with nitrate binding and reduction occurring at the molybdenum site. Whereas the flavin modifier, DPI, inhibited NADH-stimulated nitrite generation, nitrite generation stimulated by xanthine or DBA was unaffected. Thus, while xanthine or DBA directly reduces the molybdenum center, NADH initially reduces the flavin, which subsequently transfers electrons to the molybdenum.

It was previously reported that the rates of NO generation from reduction of nitrate followed Michaelis−Menten kinetics, giving apparent K_m and V_{max} values of 0.29 mM and 0.97 nmol min^{-1} mg^{-1} (*14*). However, in our studies with NADH as substrate, we clearly observed that NO generation rates increased linearly for as long as 2 h until limited by the consumption of the nitrate or reducing substrates (Figure 10). Meanwhile nitrite generation rates quickly reached a steady state, and nitrite production followed classic Michaelis−Menten kinetics with a K_m value of 6.6 mM and V_{max} of 0.23 nmol s^{-1} mg^{-1} in the presence of 2 mM NADH, while a K_m value of 8.6 mM and V_{max} of 4.5 nmol s^{-1} mg^{-1} was measured in the presence of 0.5 mM DBA (Figures 4 and 5). Our data suggested that in the process of XO-mediated nitrate reduction there are two consecutive steps: first, the reduction of nitrate to nitrite, and second, further reduction of nitrite to NO. In systems with high initial nitrate concentration and much lower levels of nitrite, production of nitrite is much faster than its consumption caused by production of NO, and thus we observe a prolonged period of nitrite accumulation, which in turn causes gradual acceleration of NO generation.

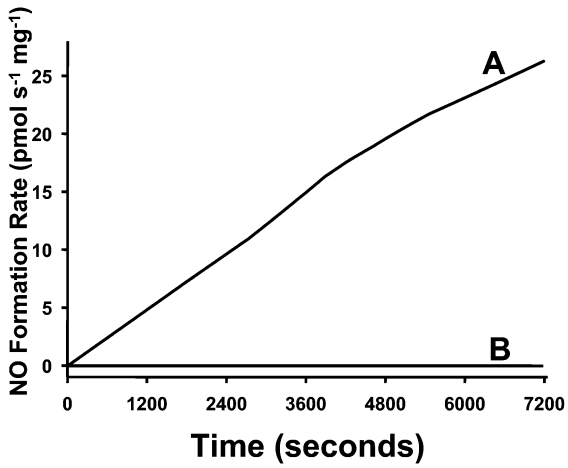

FIGURE 10: Two-hour time course of NO generation from XO-catalyzed nitrate reduction. Measurements were performed using a chemiluminescence NO analyzer under anaerobic conditions at 37 °C in PBS, pH 7.4. Time courses of NO generation were measured from (A) 5.0 mM NADH and 10.0 mM nitrate in the presence of 0.1 mg/mL XO and (B) 5.0 mM NADH and 10.0 mM nitrate.

Although xanthine was an efficient reducing substrate of XO-catalyzed nitrite reduction, excessive xanthine exerted inhibition of NO production. Furthermore, we also observed that the presence of excess NADH (>10 mM) or DBA (>2 mM) had no inhibitory effect on XO-catalyzed NO generation. Our results further prove that excessive xanthine acts to inhibit XO by binding to the molybdenum site of the reduced enzyme, as reported previously (*27*, *28*), thus blocking the binding of nitrate as well as nitrite at this enzyme site.

It has been reported that purine and aldehyde substrate hydroxylation takes place via a base-catalyzed mechanism and that these substrates must be deprotonated for hydroxylation (*15*). The rate of XO reduction by purine and aldehyde greatly increases when the pH value is increased from 6.0 to 8.0, and this increased rate of XO reduction would be expected to increase the rate of nitrate reduction. However, our experiments showed that acidic conditions promote XO-catalyzed nitrate reduction to nitrite and nitrite to NO. Both rates of nitrite and NO generation increased, as the pH was decreased from 8.0 to 5.0. This suggests that nitrate reduction likely takes place via an acid-catalyzed mechanism. Indeed, we have reported that XO-mediated nitrite reduction also takes place via an acid-catalyzed mechanism, presumably due to nitrite protonation (*16*). However, XO-mediated nitrate reduction also takes place via an acid-catalyzed mechanism despite the fact that NO_3^- is a strong acid that would not be significantly protonated by changing pH over the range from 8 to 5.0. This suggests that the protonation of a specific site of the enzyme may be responsible for facilitating the process of nitrate and nitrite reduction.

From the studies performed, it is clear that XO can catalyze the process of nitrite and NO generation from nitrate under anaerobic or markedly hypoxic conditions similar to those occurring in ischemic tissues. The key questions are the following: what is the magnitude of this process; and are

the levels of nitrite and NO produced likely to have functional significance? To address these critical questions, a kinetic model can be constructed that enables prediction of the magnitude of XO-catalyzed nitrite and NO formation and understanding the quantitative importance of this mechanism of nitrite and NO generation in biological systems. On the basis of typical Michaelis−Menten kinetics of XO catalyzed nitrite generation from nitrate reduction and NO generation from nitrite reduction, the following equations would define the steps in the reaction mechanism:

$$E_{ox} + S \underset{K_{-1}}{\overset{K_1}{\rightleftharpoons}} E_{ox}\cdot S \xrightarrow{K_2} E_{red} + P \quad (1)$$

$$E_{red} + \text{Nitrate} \underset{K_{-3}}{\overset{K_3}{\rightleftharpoons}} E_{red}\cdot\text{Nitrate} \xrightarrow{K_4} E_{ox} + \text{Nitrite} \quad (2)$$

$$E_{red} + \text{Nitrite} \underset{K_{-5}}{\overset{K_5}{\rightleftharpoons}} E_{red}\cdot\text{Nitrite} \xrightarrow{K_6} E'_{red} + NO \quad (3)$$

$$E'_{red} + \text{Nitrite} \underset{K_{-8}}{\overset{K_7}{\rightleftharpoons}} E'_{red}\cdot\text{Nitrite} \xrightarrow{K_8} E_{ox} + NO \quad (4)$$

where E_{ox} is the fully oxidized enzyme, E_{red} is the two-electron reduced enzyme, and E'_{red} is the one-electron reduced enzyme. S refers to the reducing substrates of XO, such as xanthine, and P is the corresponding product. It should be noted that for each xanthine oxidized, one molecule of nitrate could be reduced to nitrite, or two molecules of nitrite could be reduced to NO. The total enzyme concentration, $[E_t]$, can be defined as follows:

$$E_t = [E_{ox}] + [E_{ox}S] + [E_{red}] + [E_{red}\text{nitrate}] + [E_{red}\text{nitrite}] + [E'_{red}] + [E'_{red}\text{nitrite}] \quad (5)$$

At the beginning of the incubation, nitrite concentration is zero; therefore, eqs 3 and 4 can be ignored and eq 5 can be simplified to yield eq 6:

$$E_t = [E_{ox}] + [E_{ox}S] + [E_{red}] + [E_{red}\text{nitrate}] \quad (6)$$

From eqs 1, 2, and 6, the rate of nitrite generation during the beginning of the incubation can be derived, and this can be expressed in the form of the Michaelis−Menten equation

$$V_{[NO_2^-]} = \frac{k_{cat}[E_t][S]}{K_m + [S]} \quad (7)$$

where terms are defined as follows:

$$k_{cat} = \frac{[NO_3^-]}{\frac{k_{-3}+k_4}{k_3k_4} + \left(\frac{1}{k_2}+\frac{1}{k_4}\right)[NO_3^-]}$$

$$k_m = \frac{\frac{k_{-1}+k_2}{k_1k_2}[NO_3^-]}{\frac{k_{-3}+k_4}{k_3k_4} + \left(\frac{1}{k_2}+\frac{1}{k_4}\right)[NO_3^-]}$$

As can be seen in Figure 4, under conditions with high initial nitrate concentration and reducing substrates, the nitrite generation quickly reaches a steady state, and substrate-dependent nitrite generation rates are precisely fit by eq 7 (correlation coefficient $\gamma^2 > 99\%$). Under conditions where the accumulated nitrite concentration (μM) is far below its K_m (2−3 mM) for XO, the rate of NO generation from XO mediated nitrite reduction linearly increases with the linear increase in nitrite concentration (Figure 3.) This confirms that in the process of XO mediated nitrate reduction there are two consecutive steps: first, the reduction of nitrate to nitrite; and second, further reduction of nitrite to NO.

To consider the inhibitory effect of xanthine on nitrite generation, another equation must be considered

$$E_{red} + X \underset{K_{-9}}{\overset{K_9}{\rightleftharpoons}} E_{red}^{\cdot}X \quad (8)$$

Despite the effect of nitrite in the system, the total enzyme concentration $[E_t]$ can be simplified as follows:

$$E_t = [E_{ox}] + [E_{ox}S] + [E_{red}] + [E_{red}\text{Nitrate}] + [E_{red}X] \quad (9)$$

The rate of nitrite generation can be expressed as follows:

$$V_{[NO_2^-]} = \frac{V_{max}}{1 + k_m/[X] + [X]/k_i} \quad (10)$$

where

$$V_{max} = \frac{[E_t][NO_3^-]}{\frac{k_{-3}+k_4}{k_3k_4} + \left(\frac{1}{k_2}+\frac{1}{k_4}\right)[NO_3^-]}$$

$$k_m = \frac{\frac{k_{-1}+k_2}{k_1k_2}[NO_3^-]}{\frac{k_{-3}+k_4}{k_3k_4} + \left(\frac{1}{k_2}+\frac{1}{k_4}\right)[NO_3^-]}$$

$$k_i = \frac{\frac{k_{-3}+k_4}{k_3k_4} + \left(\frac{1}{k_2}+\frac{1}{k_4}\right)[NO_3^-]}{\frac{(k_{-3}+k_4)k_9}{k_3k_4k_{-9}}}$$

It was observed that over a broad range of physiological nitrate concentrations from 0.1 to 1 mM, eq 10 provided a good fit to the experimental data measuring the rate of nitrite generation from XO in the presence of xanthine (Figure 6).

With a few exceptions, such as pepsin and alkaline phosphatase, most mammalian enzymes are active only at pH values in the range 5−9. Studies of the pH dependence of XO-catalyzed nitrate generation showed that both nitrate reduction to nitrite and further nitrite reduction to NO took place via an acid-catalyzed mechanism. In our previous study of pH effects on XO-catalyzed NO generation by nitrite reduction, we suggested that protonated nitrite (HNO_2) might directly bind to reduced XO. However, nitrate is not readily protonated upon decreasing the pH decrease from pH 8 to pH 5. Therefore, protonation of a functional group of XO under acidic conditions may be the cause of the increased activity of nitrate and nitrite reduction seen with lowering of the pH to 5, while the loss of activity at lower pH values

is likely due to denaturation of the enzyme that would occur under strongly acidic conditions.

It has been previously demonstrated that the activity of XO in the postischemic rat heart is 16.8 millunits/g of protein (*30*), which corresponds to 0.013 mg of XO/g of protein or ~3.4 μg/g of cell water. The total XO and xanthine dehydrogenase (XDH) activity, however, is 10-fold above this value, and it has been reported that when the enzyme is treated with dithioerythritol, conversion from the oxidase to the dehydrogenase form occurs and is accompanied by an increase in nitrate reductase activity (*24*). Nitrate concentration in blood or tissues is highly variable with 20−100 μM levels observed under normal physiological conditions and is markedly increased reaching 400−500 μM levels under pathological conditions (*31*). After treatment with NO-donating vasodilator drugs, nitrate levels can be further elevated reaching mM values (*25*). In the ischemic heart, xanthine levels rise from near zero to values on the order of 10−100 μM and nitrate levels up to ~100−500 μM (*30*, *31*). At normal pH values of 7.4, the rate of XO-catalyzed nitrate reduction to nitrite would be as much as 1 nM/s. During myocardial ischemia, marked acidosis occurs with intracellular pH rapidly falling to less than 6.0 within 10 min following the onset of global ischemia (*10*, *32*). When pH decreases to 6.0, the rate of XO-catalyzed nitrate reduction would be estimated to increase to 1.5 nM/s and, at pH 5, to 3 nM/s, which means that nitrite levels up to ~2 μM would be produced within 10 min. In rat hearts, XDH concentration is 5−10 times higher than the concentration of XO (*30*). Thus, it is likely that overall production of nitrite and NO from xanthine oxidoreductase could be 10 times higher than that from XO alone, so that nitrite levels of up to 20 μM could be produced over a 10−20 min period of no-flow global ischemia accompanied by marked hypoxia and acidosis (*10*, *30*). These levels of nitrite are sufficient to result in rates of NO generation comparable to that from maximally activated NOS (*16*). While the rate of XO-mediated nitrate and nitrite reduction with NO formation is accelerated by the conditions of acidosis occurring during ischemia, this acidosis has been shown to result in reversible denaturation of NOS, which progresses to irreversible denaturation and enzyme degradation (*33*). Thus, XOR-catalyzed nitrate reduction to nitrite with further reduction to NO could be an important source of NO generation in ischemic tissues such as the heart. NO derived from nitrate and nitrite would accumulate during ischemia. Initially, it could serve to provide protection via compensatory vasodilatation, whereas upon reperfusion it would react with superoxide, forming peroxynitrite, which can result in protein nitration and cellular injury (*34*, *35*).

Overall, it is clear that XOR-mediated nitrate and nitrite reduction can potentially be an important source of NO under ischemic conditions in biological tissues that contain substantial levels of the enzyme along with nitrate or nitrite and reducing substrates for the enzyme. In tissues such as the liver and gastrointestinal tract, which contain high levels of XOR, this could be even more pronounced than for the example of the heart considered above (*36*). Beyond the obligatory need for the enzyme, the levels of tissue nitrate and nitrite and enzyme reducing substrates have a critical role in controlling this process. Nitrate and nitrite are required, and overall are the most limiting substrates. The K_m measured for nitrate was in the range of 6−9 mM, with NADH or DBA as substrates whereas typical tissue levels of nitrate are 1−2 orders of magnitude below this value. Similarly for nitrite, high K_m values of about 2 mM have been measured (*16*). A number of factors that increase tissue nitrate or/and nitrite levels, such as inflammatory conditions with prior activation of constitutive or inducible NOS, dietary sources, pharmacological sources, or bacterial sources, could all modulate this pathway of NO generation. This pathway also requires a reducing substrate, such as NADH or xanthine. If particularly high levels of xanthine accumulate, however, this pathway would be inhibited and this may serve a regulatory function to prevent overproduction of NO. Thus, XOR can be an important source of NOS-independent NO generation. Under anaerobic conditions, XO reduces nitrate to nitrite and nitrite to NO at the molybdenum site of the enzyme; with xanthine, NADH, or aldehyde substrates serving to provide the requisite reducing equivalents. The substrate-dependent rate relationship for anaerobic nitrate reduction by XO was determined. This XO-mediated nitrate reduction to nitrite and NO could be a particularly important source of NO production under anoxic conditions where the function of NOS is impaired.

REFERENCES

1. Palmer, R. M., Ferrige, A. G., and Moncada, S. (1987) *Nature 327*, 524−526.
2. Ignarro, L. J., Byrns, R. E., Buga, G. M., and Wood, K. S. (1987) *Circ. Res. 61*, 866−879.
3. Furchgott, R. F., and Vanhoutte, P. M. (1989) *Faseb J. 3*, 2007−2018.
4. Marletta, M. A., Yoon, P. S., Iyengar, R., Leaf, C. D., and Wishnok, J. S. (1988) *Biochemistry 27*, 8706−8711.
5. Bredt, D. S., Hwang, P. M., Glatt, C. E., Lowenstein, C., Reed, R. R., and Snyder, S. H. (1991) *Nature 351*, 714−718.
6. Bredt, D. S., and Snyder, S. H. (1992) *Neuron 8*, 3−11.
7. Benjamin, N., O'Driscoll, F., Dougall, H., Duncan, C., Smith, L., Golden, M., and McKenzie, H. (1994) *Nature 368*, 502.
8. Lundberg, J. O., Weitzberg, E., Lundberg, J. M., and Alving, K. (1994) *Gut 35*, 1543−1546.
9. Lundberg, J. O., Carlsson, S., Engstrand, L., Morcos, E., Wiklund, N. P., and Weitzberg, E. (1997) *Urology 50*, 189−191.
10. Zweier, J. L., Wang, P., Samouilov, A., and Kuppusamy, P. (1995) *Nat. Med. 1*, 804−809.
11. Zweier, J. L., Samouilov, A., and Kuppusamy, P. (1999) *Biochim. Biophys. Acta 1411*, 250−262.
12. Samouilov, A., Kuppusamy, P., and Zweier, J. L. (1998) *Arch. Biochem. Biophys. 357*, 1−7.
13. Zhang, Z., Naughton, D., Winyard, P. G., Benjamin, N., Blake, D. R., and Symons, M. C. (1998) *Biochem. Biophys. Res. Commun. 249*, 767−772.
14. Millar, T. M., Stevens, C. R., Benjamin, N., Eisenthal, R., Harrison, R., and Blake, D. R. (1998) *FEBS Lett. 427*, 225−228.
15. Godber, B. L., Doel, J. J., Sapkota, G. P., Blake, D. R., Stevens, C. R., Eisenthal, R., and Harrison, R. (2000) *J. Biol. Chem. 275*, 7757−7763.
16. Li, H., Samouilov, A., Liu, X., and Zweier, J. L. (2001) *J. Biol. Chem. 276*, 24482−24489.
17. McCord, J. M., Roy, R. S., and Schaffer, S. W. (1985) *Adv. Myocardiol. 5*, 183−189.
18. Allison, R. C., Kyle, J., Adkins, W. K., Prasad, V. R., McCord, J. M., and Taylor, A. E. (1990) *J. Appl. Physiol. 69*, 597−603.
19. Zweier, J. L., Broderick, R., Kuppusamy, P., Thompson-Gorman, S., and Lutty, G. A. (1994) *J. Biol. Chem. 269*, 24156−24162.
20. Zweier, J. L., Kuppusamy, P., and Lutty, G. A. (1988) *Proc. Natl. Acad. Sci. U.S.A. 85*, 4046−4050.
21. Dixon, M., and Thurlow, S. (1924) *Biochem. J. 18*, 989−992.
22. Westerfeld, w. W., Bichert, D. A., and Higgins, E. S. (1959) *J. Biol. Chem. 234*, 1897−1900.
23. Fridovich., I., and Handler., P. (1962) *J. Biol. Chem. 237*, 916−921.

24. Sergeev, N. S., Ananiadi, L. I., L'Vov N, P., and Kretovich, W. L. (1985) *J. Appl. Biochem. 7*, 86−92.
25. Schneeweiss, A., and Weiss, M. (1990) in *Advances in Nitrate Therapy*, Second, Revised and Enlarged Edition ed., Springer-Verlag, Berlin.
26. Shinobu, L. A., Jones, S. G., and Jones, M. M. (1984) *Acta Pharmacol. Toxicol. (Copenhagen) 54*, 189−194.
27. Hille, R., and Stewart, R. C. (1984) *J. Biol. Chem. 259*, 1570−1576.
28. Rubbo, H., Radi, R., and Prodanov, E. (1991) *Biochim. Biophys. Acta 1074*, 386-391.
29. Ellis, G., Adatia, I., Yazdanpanah, M., and Makela, S. K. (1998) *Clin. Biochem. 31*, 195−220.
30. Xia, Y., and Zweier, J. L. (1995) *J. Biol. Chem. 270*, 18797−18803.
31. Galley, H. F., Le Cras, A. E., Logan, S. D., and Webster, N. R. (2001) *Br. J. Anaesth. 86*, 388−394.
32. Thompson-Gorman, S. L., and Zweier, J. L. (1990) *J. Biol. Chem. 265*, 6656−6663.
33. Giraldez, R. R., Panda, A., Xia, Y., Sanders, S. P., and Zweier, J. L. (1997) *J. Biol. Chem. 272*, 21420−21426.
34. Beckman, J. S., Beckman, T. W., Chen, J., Marshall, P. A., and Freeman, B. A. (1990) *Proc. Natl Acad. Sci. U.S.A. 87*, 1620−1624.
35. Wang, P., and Zweier, J. L. (1996) *J. Biol. Chem. 271*, 29223−29230.
36. Sarnesto, A., Linder, N., and Raivio, K. O. (1996) *Lab. Invest. 74*, 48−56.

BI026385A